Journal of Thermal Analysis, Vol. 46 (1996) 1223-1238

KINETICS OF THERMAL DEHYDROXYLATION OF ALUMINOUS GOETHITE

H. D. Ruan and R. J. Gilkes

Soil Science and Plant Nutrition, Faculty of Agriculture, University of Western Australia, Nedlands, WA 6907, Australia

(Received January 11, 1995)

Abstract

The kinetics of dehydroxylation of synthetic aluminous goethite was studied using isothermal and non-isothermal thermogravimetry. The complete isothermal dehydroxylation can be described by the Johnson-Mehl equation with up to three linear regions in plots of $\ln\ln [1/(1-y)]$ *vs.* $\ln t$. Kinetics for the initial stage of dehydroxylation changed from diffusion to first-order through the temperature range 190 to 260°C. The rate of dehydroxylation was reduced by Al-substitution and increased with temperature. Activation energy for dehydroxylation, calculated from the time to achieve a given dehydroxylation extent, varied depending on the extent of dehydroxylation and Al-substitution. Non-stoichiometric OH existed in goethite and some remained in hematite after the complete crystallographic transition.

Keywords: dehydroxylation, goethite, hematite, kinetics

Introduction

Dehydroxylation of goethite (α-FeOOH) to form hematite can be described by the reaction: $2\alpha\text{-FeOOH} \rightarrow \alpha\text{-Fe}_2\text{O}_3 + \text{H}_2\text{O}$. This dehydroxylation process, has been described by both homogeneous and heterogeneous models [1–5] where simultaneous loss of water from all parts of the lattice is distinguished as a homogeneous mechanism and the localised loss of oxygen ions, cation migration and changes of oxygen packing as a heterogeneous mechanism [2, 6]. Dehydroxylation reactions may obey either the first-order law [7–9] or follow a diffusion model [10–11]. Brindley *et al.* [11] demonstrated that most experimental observations of first-order kinetics can be re-interpreted in accordance with a diffusion-controlled kinetic law. Goss [12] found that the dehydroxylation of goethite is phase-boundary controlled at high temperatures and the mechanism is more complex at lower temperatures and at early stages.

Most research on the dehydroxylation process has focussed on ideal non-substituted goethite whereas goethite in the natural environment contains appreciable aluminium as an isomorphous substitution. Goethite may also contain excess non-stoichiometric water. Dehydroxylation of goethite can be influenced

0368–4466/96/ $ 5.00

John Wiley & Sons, Limited
Chichester

by Al-substitution [13–14] and particle size [15]. Goss [12] found that the retention of water within the porous structure of partially dehydroxylated goethite is an important control of the transformation to hematite. Goethite, formed from the ferrous system, usually contains more excess structural water (non-stoichiometric OH) and hence has a lower dehydroxylation temperature than goethite synthesized from the ferric system [16]. This excess water will affect the crystallization of hematite. Aluminium substitution in goethite is common in nature and is considered an important factor in controlling the stability of the lattice, affecting both the decomposition of the crystal structure and the rate of cation migration [17]. The present study deals with the dehydroxylation of synthetic Al-substituted goethite an elucidates the kinetics of this reaction through identifying and appropriate kinetic model.

Materials and methods

The details of experimental procedures and the characteristics of four synthetic Al-goethites formed from the ferrous system have been described elsewhere [18].

Thermal analysis

Thermogravimetric analyses (TG) and differential thermogravimetric analyses (DTG) were carried out using a Perkin-Elmer TGS-2 instrument. The isothermal dehydroxylation curves were obtained from TG. Approximately 10 mg of sample was preheated at 110°C to remove adsorbed water until weight was constant. Then the sample was heated at a rate of 80°C min^{-1} from 110°C to the desired temperature (190, 200, 210, 220, 230, 240 250 and 260°C) in flowing air and was then maintained at this temperature for up to 4 h. Weight loss obtained at time intervals was calculated as a percentage of the total weight loss measured at 260°C.

Non-isothermal dehydroxylation curves were obtained from DTG and TG traces. Approximately 10 mg of sample was heated in flowing air to 620°C at 10°C min^{-1}. Samples were preheated at 110°C for about 10 min to remove adsorbed water. The temperature of dehydroxylation maximum was obtained from the DTG output and weight loss at each temperature was calculated from the TG curves and assumed to be H_2O. Four replicates of non-isothermal analyses were made for each sample and the mean values and standard deviations were calculated.

Results and discussion

Characteristics of goethites

A brief description of characteristics of goethites is shown in Table 1. The samples were pretreated with oxalate solution to remove amorphous Fe com-

Table 1 Characteristics of goethite (Gt) synthesized from the ferrous system

Al-substitution/	UCD[1] of goethite/			$MCL^2_{Gt\ 110}$/	$MCL_{Gt\ 020}$/	Surface area/
mol%	*a*/Å	*b*/Å	*c*/Å	nm	nm	$m^2\ g^{-1}$
0	4.635(7)	9.944(4)	3.030(3)	6.4	8.9	147
9.7	4.630(9)	9.914(5)	3.017(3)	8.5	7.5	163
19.7	4.624(12)	9.867(7)	3.001(5)	8.1	5.7	208
30.1	4.619(12)	9.862(7)	2.992(4)	7.5	5.4	228

[1]UCD=unit cell dimensions; ( )=S. D.

[2]MCL=mean coherence length derived from XRD line broadening of the 110 and 020 reflections, respectively.

pounds. Goethite consisted of small crystals with surface area from 147 to 228 $m^2\ g^{-1}$. Unit cell dimensions decreased and surface area increased with increasing Al-substitution. Mean coherence length (MCL) along the *a*-axis, estimated from XRD line broadening, increased systematically with Al-substitution, whereas MCL along the *b*-axis increased for 0 to 9.7 mol% Al and then decreased between 9.7 and 30.1 mol% Al. Crystal sizes were about 5–9 nm and crystal morphology changed from a lath-shape to a smaller, more equant shape as Al-substitution increased [18].

Dehydroxylation isotherms

Figure 1 shows the dehydroxylation isotherms, which are plots of weight loss (%) against time, for temperatures from 190 to 260°C. The higher the aluminium content, the greater the amount of structural water in the samples with weight loss as at 260°C of 14.1, 15.1, 15.9 and 17.6 for 0, 9.7, 19.7 and 30.1 mol% Al. A constant weight was reached more quickly at higher temperatures, Al-substitution slowed the rate of weight loss (Fig. 1).

Kinetics of dehydroxylation

The dehydroxylation of Al-substituted goethite may be described by a general rate equation.

$$\frac{dy}{dt} = kf(y) \tag{1}$$

By separating the variables and integrating,

$$g(y) = kt \tag{2}$$

where y is the reaction fraction (ratio of weight loss at time t and total weight loss at 260°C after 200 min) at time t, k is the rate constant and $g(y)$ is the reaction function depending on the mechanism.

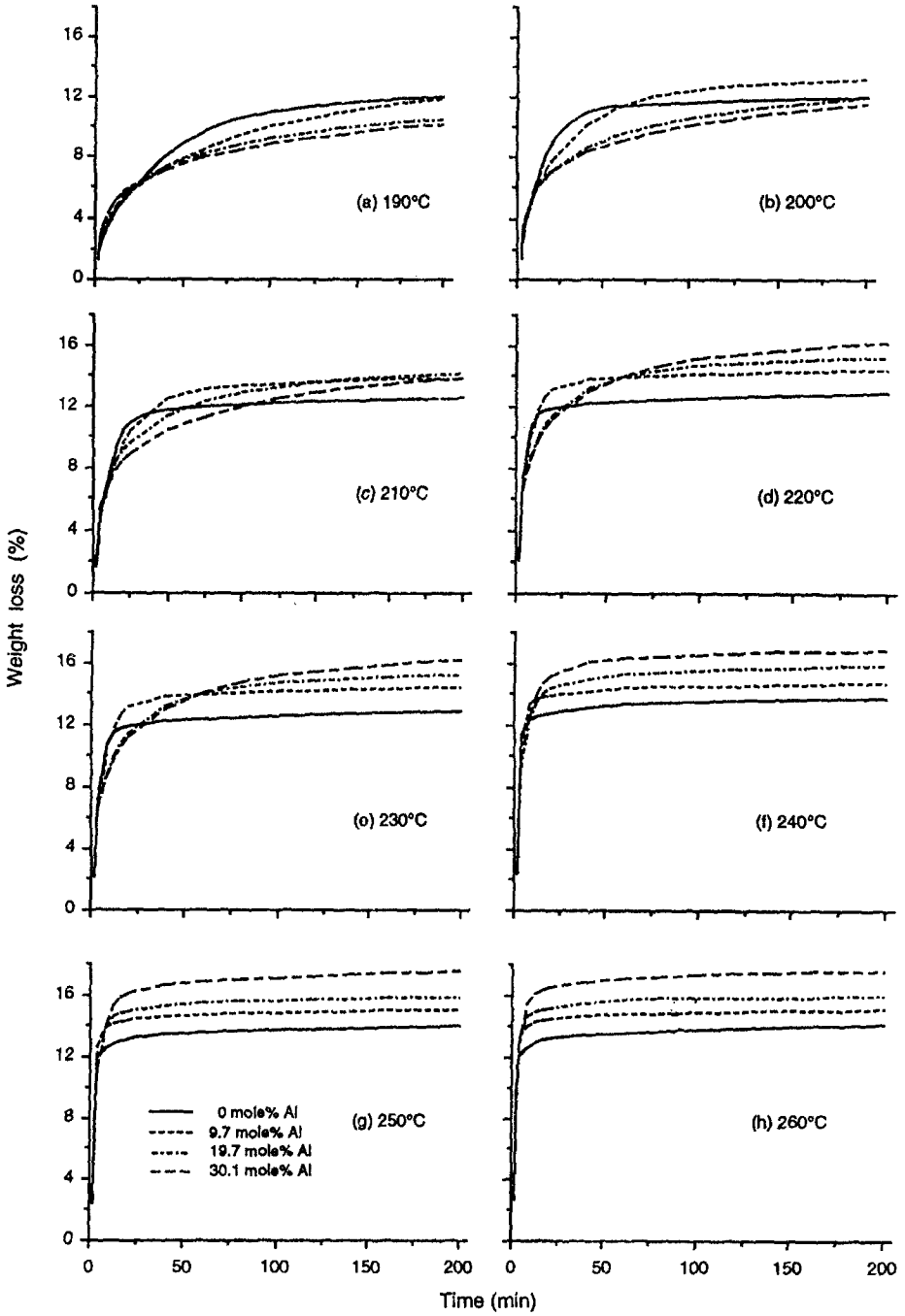

Fig. 1 Weight loss (%) for goethite *vs.* time from isothermal measurement

Plots of y *vs.* time lead to deceleratory curves [5, 11, 12].

Figure 2 shows plots of weight loss converted to reaction fraction as a function of time for 0 and 30.1 mol% Al-goethites. The total weight loss at 260°C after 200 min was assumed to represent 100% reaction.

Weight loss as a function of time can be described by the relationship

$$W_t = W_m - W_m \exp[-(kt)^n] \quad (3)$$

where W_t is the weight loss at time t, W_m is the maximum weight loss and n is an exponential factor. Dehydroxylation is complex in the solid state and the process may consist of several stages. Using $y = W_t / W_m$, Eq. (3) becomes the Johnson-Mehl or Avrami equation which is commonly used to describe isothermal kinetics [5, 12].

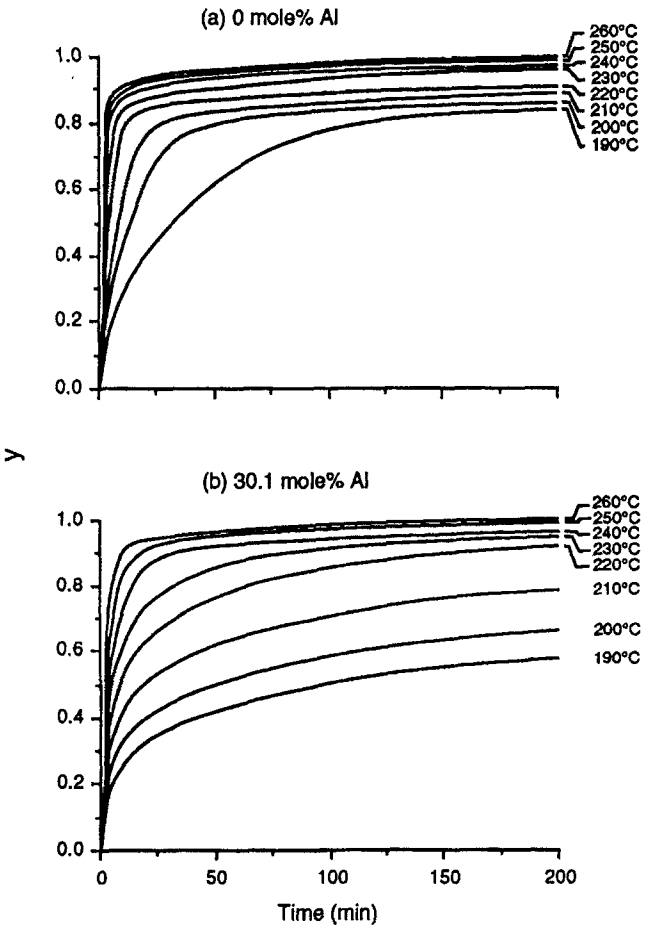

Fig. 2 Plots of dehydroxylation fraction (y) of goethite *vs.* time

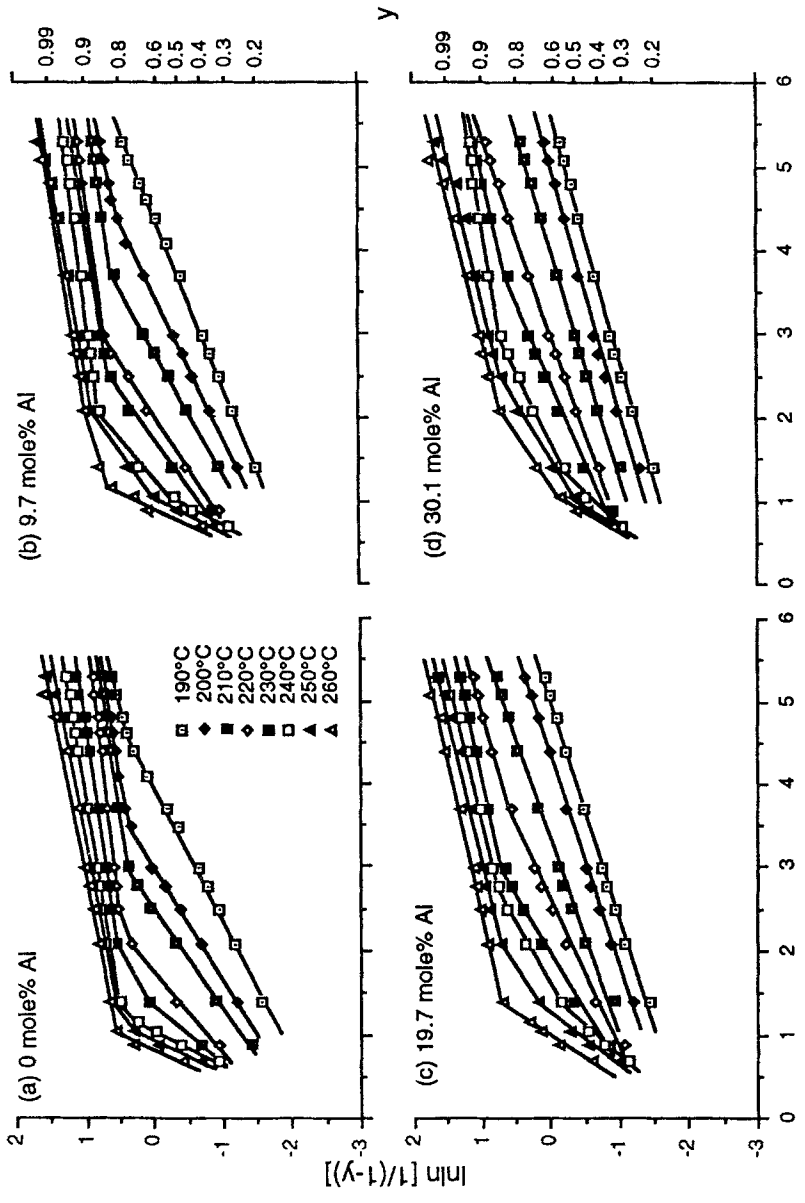

Fig. 3 The ln ln[1/(1-y)] *vs.* ln*t* plots for goethite based on the Johnson-Mehl equation showing the presence of entire linear section I, II and III for different samples and temperatures

Table 2 Data from $\ln\ln[1/(1-y)]$ *vs.* $\ln t$ plots, slopes (n) obtained for the various (I, II and III) linear portions of the plots

TG/	0 mol% Al		9.7 mol% Al		19.7 mol% Al		30.1 mol% Al	
°C	n	R^2	n	R^2	n	R^2	n	R^2
				Section I (low y values)				
190	0.627	0.997	0.494	0.999	0.374	0.997	0.338	0.997
200	0.740	0.999	0.583	1.000	0.391	0.997	0.339	0.995
210	0.852	0.996	0.653	0.999	0.418	0.992	0.359	0.996
220	1.073	0.993	0.780	0.995	0.575	0.986	0.451	0.985
230	1.489	1.000	0.905	0.990	0.700	0.988	0.519	0.987
240	2.455	0.988	2.316	0.978	1.381	0.980	1.210	0.973
250	2.963	0.990	2.617	0.991	1.625	0.969	1.773	0.973
260	2.905	0.943	2.682	0.945	1.811	0.982	2.223	0.969
				Section II (intermediate y values)				
190	0.313	0.989	–	–	–	–	–	–
200	0.304	0.975	0.277	0.988	–	–	–	–
210	0.193	0.970	0.208	0.970	–	–	–	–
220	0.434	1.000	0.167	0.974	0.349	0.993	–	–
230	0.711	1.000	0.197	0.991	0.269	0.987	0.319	0.995
240	1.193	1.000	0.994	0.977	0.660	0.993	0.553	0.996
250	0.921	1.000	0.874	0.995	0.812	1.000	0.726	0.992
260	0.238	0.982	0.390	0.909	0.276	0.994	0.842	0.989
				Section III (high y values)				
190	–	–	–	–	–	–	–	–
200	0.118	0.990	–	–	–	–	–	–
210	0.126	0.999	–	–	–	–	–	–
220	0.122	0.996	–	–	–	–	–	–
230	0.174	0.992	–	–	–	–	–	–
240	0.188	0.990	0.153	0.991	0.315	0.974	0.197	0.973
250	0.225	0.986	0.218	0.981	0.268	0.987	0.306	0.973
260	–	–	0.195	0.986	–	–	0.306	0.973

$$y = 1 - \exp[-(kt)^n] \tag{4}$$

Taking logarithms of Eq. (4), a linear equation is obtained,

$$\ln\ln\frac{1}{1-y} = n\ln k + n\ln t \tag{5}$$

A plot of lnln $[1/(1-y)]$ *vs.* ln*t* should yield a straight line with slope *n* and intercept *n*ln*k* if a single mechanism is operating.

If a single reaction operates and obeys the Johnson-Mehl equation, a set of isokinetic curves for different temperatures would have the same value of slope *n*, and thus the same gradient when plotted as lnln $[1/(1-y)]$ *vs.* ln*t* [5]. Criado *et al.* [11] and Goss [12] found that such lnln plots may often be split into several linear sections implying that several reaction types are operating.

Table 3 The reaction functions, $g(y)$, for dehydroxylation and theoretical slopes of plots of lnln $[1/(1-y)]$ *vs.* ln*t*

Mechanism	Function $g(y)$	Slope (n)
Zero order	y	1.24
R_2–phase boundary reaction, cylindrical	$1-(1-y)^{1/2}$	1.11
R_3–phase boundary reaction, spherical	$1-(1-y)^{1/3}$	1.07
F_1–random nucleation, one nucleus/particle	$-\ln(1-y)$	1.00
A_2–random nucleation, Avrami equation I	$[-\ln(1-y)]^{1/2}$	2.00
A_3–random nucleation, Avrami equation II	$[-\ln(1-y)]^{1/3}$	3.00
D_1–one-dimensional diffusion	y^2	0.62
D_2–two-dimensional diffusion, cylindrical	$(1-y)\ln(1-y)+y$	0.57
D_3–three-dimensional diffusion, spherical, Jander equation	$[1-(1-y)^{1/3}]^2$	0.54
D_4–three-dimensional diffusion, spherical, Ginstling-Brounshtein equation	$(1-2/3y)-(1-y)^{2/3}$	0.57

The experimental data for Al-goethite are plotted as lnln $[1/(1-y)]$ *vs.* ln*t* in Fig. 3. Single line fits were obtained for low temperature measurements, (i.e. 190 to 220°C for 30.1 mol% Al, 190 to 210°C for 19.7 mol% Al and 190°C for 9.7 mol% Al (Fig. 3)). Multiple linear fits described the remaining data with up to three linear sections, the corresponding slopes (*n* values) are listed in Table 2. The reaction rate equations of various solid-states cited in the literature [9, 12] are shown in Table 3 so that the nature of the reaction of the present samples can be identified. The *n* values obtained from these lnln plots are indicative of the rate-determining kinetic mechanisms and various alternatives are given in Table 3. Most of the *n* values for section I, initial linear regions (low *y* values) increased from about 0.5 to 3 as temperature increased from 190 to 260°C (Table 2). On this basis the principle dehydroxylation mechanisms for the present samples varied from diffusion to random nucleation for section I. In other words, the *n* values increased for section I as temperature increased from 190 to 260°C. For section II (intermediate *y* values), *n* values were mostly < 1 which indicates that diffusion processes dominated although some values for higher temperatures were ≈ 1, indicating that other reactions were dominant.

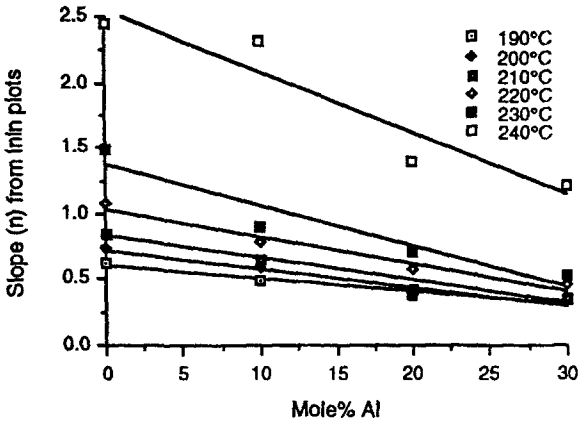

Fig. 4 Slopes (n) from lnln plots as a function of Al-substitution in goethite

The n values were small (<0.3) for section III (high y values) and do not correspond to any of the mechanistic models shown in Table 3 ($n > 0.5$).

The results of this study mostly agree with the findings of Goss [12] who indicated that the lnln plot of non-substituted goethite consisted of two linear sections and the dehydroxylation rate decreased greatly for the high y value section (>0.8, close to the y values in section III of this study). In this work, n increased systematically with increasing temperature (Table 2) and decreased with increasing Al-substitution for section I (low y values) of these plots (Fig. 4). For the II and III regions of the plots there are no significant relationships between n and mol% Al or temperature.

The time taken to achieve 50% of maximum weight loss ($t_{0.5}$) provides a single rate constant for each isotherm. Values of $t_{0.5}$, which varied between 2 and 102 min, increased with Al-substitution (Fig. 5a) and decreased with temperature (Fig. 5b). The increase in $t_{0.5}$ due to Al-substitution was much greater for a low heating temperature (e.g. 190°C) than for a high temperature (e.g. 260°C).

Activation energy

The Arrhenius plot (ln (rate constant) *vs.* $1/T$) is generally linear and may be used to calculate the activation energy (E_a) of reaction; in some cases, however, the plots of these experimental data are curved, as has also been reported by Goss [12]. The disadvantage of this method, which fails to consider any variation in activation energy as a function of the reaction fraction, y, has been discussed by Redfern [5]. He suggested that activation energy must be determined independently of the empirical function $g(y)$, so that any change in the kinetic-controlling mechanism during dehydroxylation can be observed. The time to a given dehydroxylation fraction ('time to') method has therefore been proposed [5, 12]. By rewriting Eq. (1), the time t_Y, for the reaction function $g(y)$ where $y=Y$ (of value 0 to 1), the expression becomes:

$$t_Y = k^{-1} \int_0^Y f^{-1}(y)dy \tag{6}$$

Values of t_Y (in minutes) were collected for a series of temperatures corresponding to different values of y. Provided that $f(y)$ does not vary over the limited temperature range considered, the integral is constant. Thus t_Y is proportional to k^{-1}, and from the Arrhenius equation [5],

$$k = A \exp(-E_a/RT) \tag{7}$$

$$t_Y \propto A^{-1} \exp(E_a/RT) \tag{8}$$

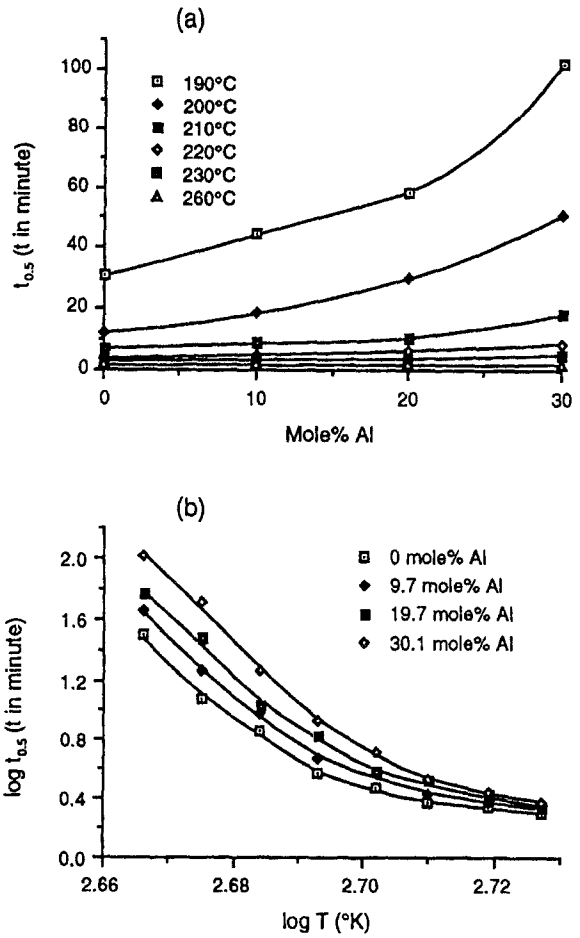

Fig. 5 Plots of $t_{0.5}$ taken from TG curves for goethite *vs.* Al-substitution (a) and temperature (b)

$$\ln t_Y = \text{constant} - \ln A + E_a/RT \quad (9)$$

Plots of $\ln t_Y$ *vs.* $1000/T$ are shown in Fig. 6.

Activation energy at each value of y can be obtained from the instantaneous slope E_a/R. The slope of the lines thus varies with both temperature and Al-substitution, and increases with increasing fraction of dehydroxylation, y (Fig. 6). The advantage of the 'time to' method over the Avrami-Erofe'ev-Johnson-Mehl approach is that it does not depend on defining a specific function $g(y)$ and is thus capable of indicating when activation energy is a function of y [12].

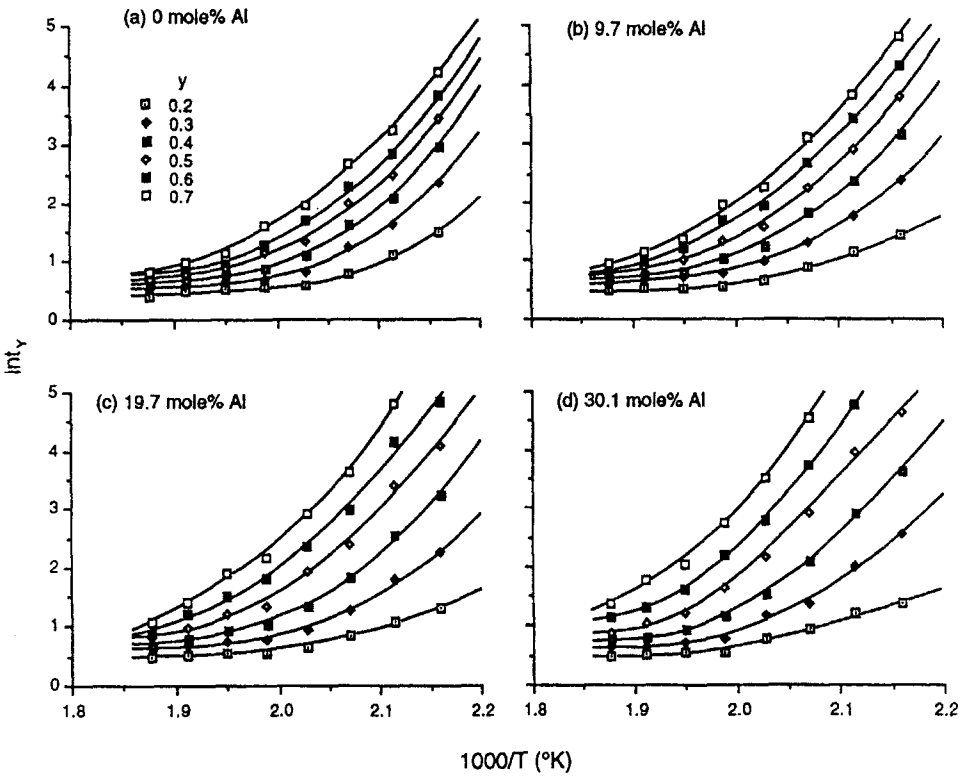

Fig. 6 $\ln t_Y$ *vs.* $1000/T$ for values of dehydroxylation fraction (y) from 0.2 to 0.7 for goethite

The activation energies, at several values of y, calculated from the instantaneous slope of the ln 'time to' plots for selected temperature groups, are shown in Table 4. The increase in activation energy with increasing y is probably due to dehydroxylation kinetics being controlled by different mechanisms at different stages of dehydroxylation. The activation energies obtained from the 'time to' method indicate that dehydroxylation at low temperatures, which dominantly obeyed a diffusion law, corresponded to a high activation energy whereas dehydroxylation at high temperatures, which mainly followed a first-order mechanism, corresponded to a lower activation energy (Table 4). This is consistent

with the changes in n, the order of kinetic reaction, identified from the lnln plots as mentioned before (Table 2). Al-substitution considerably increased the activation energy for $y > 0.4$ (Table 4).

The relationship between activation energy and fraction of reaction (dehydroxylation), y, is affected by Al-substitution (Table 4). Figure 7 shows that activation energy increases linearly with y for the heating temperature range

Table 4 Activation energy (E_a) for dehydroxylation calculated from ln 'time to' method for synthetic goethite as affected by aluminium substitution

		E_a/kJ mol^{-1}					
y	mol%/ Al	190, 200, 210°C*	200, 210 220°C	210, 220 230°C	220, 230 240°C	230, 240 250°C	240, 250 260°C
0.2	0	66	49	25	7	5	13
	9.7	49	47	34	12	6	4
	19.7	42	43	29	9	4	6
	30.1	40	39	40	25	3	6
0.3	0	103	79	57	20	11	13
	9.7	98	74	53	29	16	13
	19.7	89	83	50	23	10	11
	30.1	108	80	58	49	14	6
0.4	0	124	97	79	33	20	18
	9.7	125	109	79	44	31	16
	19.7	129	117	81	41	21	30
	30.1	144	133	93	64	36	17
0.5	0	133	111	87	49	40	21
	9.7	142	131	95	59	50	24
	19.7	156	145	105	75	39	45
	30.1	157	173	129	98	68	40
0.6	0	142	113	104	73	45	23
	9.7	151	145	101	73	76	45
	19.7	172	173	119	90	62	72
	30.1	198**	192	156	123	94	54
0.7	0	146	124	108	87	68	34
	9.7	159	152	116	90	91	49
	19.7	220**	184	150	107	82	92
	30.1	–	209	183	155	110	76

*Instantaneous slope obtained from these three temperatures for calculation of activation energy
**Two temperatures only

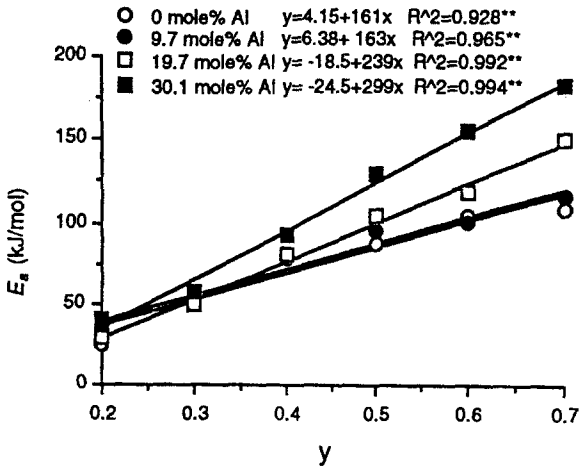

Fig. 7 Activation energy (E_a) for the temperature range 210–230°C as a function of dehydroxylation fraction (y) for Al-goethites

210–230°C. Activation energy values are similar for all four goethites for $y=0.2$~0.3 but activation energy increases with Al content for higher values of y (Table 4). The graphs of activation energy *vs.* y for temperature ranges lower than 210–230°C have deceleratory shapes (not shown), associated with the de-

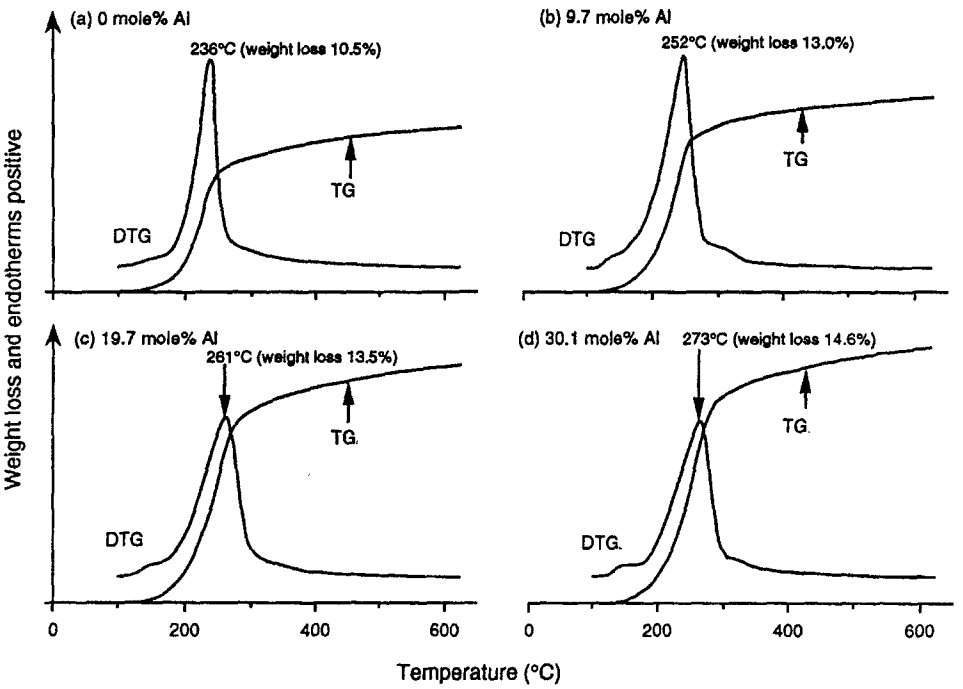

Fig. 8 Non-isothermal thermogravimetric graphs (TG and DTG) for Al-goethite

hydroxylation mechanism changing from dominantly diffusion to a first-order reaction. The graphs of activation energy *vs.* y for temperature ranges higher than 210–230°C have acceleratory shapes (not shown). The changes in activation energy with reaction fraction and temperature reflect changes in the mechanisms of dehydroxylation and which are related to changes in the characteristics of the solid phase during the transformation of goethite to hematite. These changes include effects on crystal size, crystal morphology, unit cell parameters, specific surface area and microporosity which are associated with the loss of structural water, migration of Fe and Al and reorganisation of oxygen packing.

Non-isothermal analysis

Figure 8 shows that the temperature of dehydroxylation maximum obtained from DTG curves increased with increasing Al-substitution. The amounts of weight loss were 10.5, 13.0, 13.5 and 14.6% corresponding to DTG maxima of 236, 252, 261 and 273°C and total amounts of weight loss at 620°C were 16.0, 18.0, 19.0 and 20.3% for 0, 9.7, 19.7 and 30.1 mol% Al, respectively (Fig. 8). A small peak at temperatures between 150 and 200°C of the DTG curves may indicate the weakly bound non-stoichiometric OH in goethite or minor amount of amorphous Fe oxide although little of this should have been present in the samples after oxalate extraction. The continuing weight loss at temperature above 350°C in the TG curves represents retained water being released from hematite (Fig. 8). Pollack *et al.* [18–19] proposed that the extent of retention of non-stoichiometric OH in the goethite structure is a consequence of the dehydroxylation mechanism followed.

By calculating the ideal water content of Al-goethite using the equation,

$$2Fe_{1-x}(Al_x)OOH = [Fe_{1-x}(Al_x)]_2O_3 + H_2O \qquad (10)$$

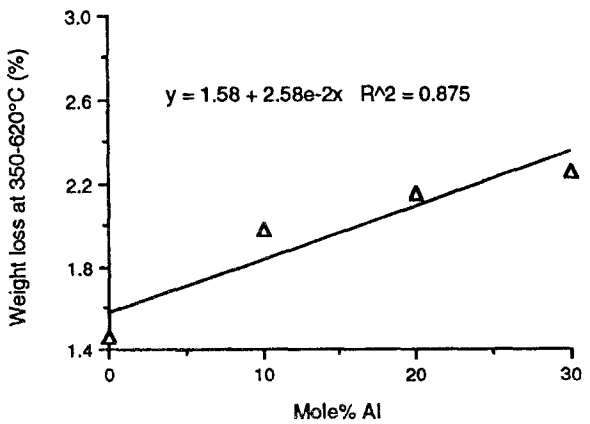

Fig. 9 Weight loss for the temperature range 350–620°C (i.e. excess water) *vs.* Al-substitution in goethite

the total theoretical amounts of structural water were 10.1, 10.4, 10.8 and 11.4% for 0, 9.7, 19.7 and 30.1 mol% Al.

The excess water (lost for temperature 350–620°C) in the present samples can then be estimated and was 1.5, 2.0, 2.2 and 2.3%. This excess water is linearly related to Al content (Fig. 9) so that it is possible that Al^{3+} retains combined OH more energetically than does Fe^{3+}, perhaps due to the higher ionic potential of Al^{3+}. For this reason greater amounts of chemisorbed surface water and non-stoichiometric OH are associated with synthetic Al-goethite [14, 16, 18].

Surface area and crystal size reflect the effect of Al-substitution on crystal properties. Consequently these properties are related to the excess water content of goethite and hydrohematite. Plots of weight loss (110–620°C) as a function of surface area and MCL derived from the XRD 020 reflection of goethite are shown in Fig. 10 and demonstrate strong linear relationships. Water content of goethite is positively related to surface area and negatively related to crystal

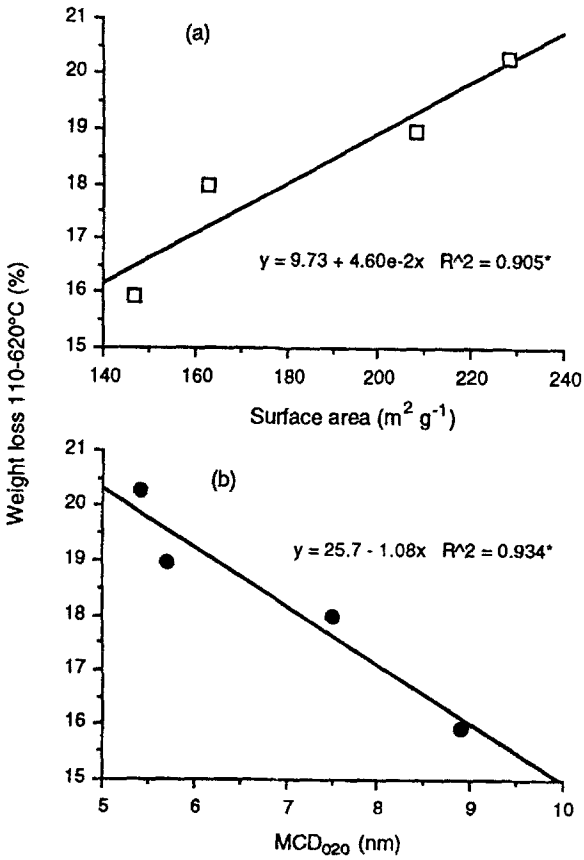

Fig. 10 Weight loss (%, 110–620°C) as a function of (a) surface area and (b) mean coherence length derived from the XRD 020 line, for Al-goethite

size. Wolska and Schwertmann [21] also found that non-stoichiometric OH can remain in the hematite structure after dehydroxylation of goethite and described this material as hydrohematite (α–$Fe_{2-x/3}O_{3-x}OH_x$).

Conclusions

The dehydroxylation kinetics of Al-substituted goethite reflect different mechanisms that operate at different temperatures and at different reaction fractions (y) but the kinetics can be described by the Johnson-Mehl model with between one and three linear portions. For the low y section (i.e. section I) of the lnln plot (Johnson-Mehl equation), the kinetic mechanism appears to change from dominantly diffusion to random nucleation as indicated by increases in the value of the order of reaction (n) which increases as temperature increases and decreases as Al-substitution increases. For intermediate y values (i.e. section II of the lnln plot), diffusion appears to be the dominant mechanism. For high y values of the lnln plot, values of n do not correspond to any of the kinetic mechanisms cited in literature and the reactions may reflect the several processes involved in the loss of excess water, migration of cations and rearrangement of oxygen packing in the structure of hematite.

References

1 G. W. Brindley and M. Nakahira, J. Am. Ceram. Soc., 42 (1959) 311–314, 314–418, 319–324.
2 H. F. W. Taylor, Clay Miner. Bull., 5 (1962) 45.
3 J. B. Holt, I. B. Cutler and M. E. Wadsworth, J. Am. Ceram. Soc., 45 (1962) 133.
4 F. Toussaint, J. J. Fripiat and M. C. Gastuche, J. Phys. Chem., 67 (1963) 26.
5 S. A. T. Redfern, Clay Miner., 22 (1987) 447.
6 H. F. W. Taylor, Clays Clay Min. Proc. 12th Conf., Pergamon Press, 1964, p. 9–10.
7 E. B. Allison, Silicates Ind., 19 (1954) 363.
8 P. Murray and J. White, Trans. Brit. Ceram. Soc., 54 (1955) 137.
9 J. D. Hancock and J. H. Sharp, J. Am. Ceram. Soc., 55 (1972) 74.
10 G. W. Brindley, J. H. Sharp, J. H. Patterson and B. N. Narahari, Am. Miner., 52 (1967) 201.
11 J. M. Criado, A. Ortega, C. Real and E. Torres de Torres, Clay Miner., 19 (1984) 653.
12 C. J. Goss, Miner. Mag., 51 (1987) 437.
13 K. Jónás and K. Solymár, Acta Chim. Acad. Sci. Hung., 66 (1970) 383.
14 M. B. Fey and J. B. Dixon, Clays Clay Miner., 29 (1981) 91.
15 R. C. Mackenzie and G. Berggren, Differential Thermal Analysis 1, Academic Press, 1970, p. 271–302.
16 D. G. Schulze and U. Schwertmann, Clay Miner., 19 (1984) 521.
17 I. Rozenson and L. Heller-Kállai, Clays Clay Miner., 28 (1980) 391.
18 H. D. Ruan and R. J. Gilkes, Clay Clay Miner., 43 (1995) 196.
19 J. B. Pollack, D. Pitmen, B. N. Khare and C. Sagan, J. Geophysical Research, 75 (1970) 7481.
20 J. B. Pollack, R. N. Wilson and G. G. Goles, J. Geophysical Research, 75 (1970) 7491.
21 E. Wolska and U. Schwertmann, Z. Kristallographie, 189 (1989) 223.